

# HIGGS $\mathcal{CP}$ FROM $H/A^0 \rightarrow \tau\tau$ DECAY \* \*\*

MAŁGORZATA WOREK

Institut für Theoretische Teilchenphysik (TTP)  
Universität Karlsruhe, D-76128 Karlsruhe, Germany.

Institute of Physics, University of Silesia  
Uniwersytecka 4, 40-007 Katowice, Poland.  
e-mail: Malgorzata.Worek@ifj.edu.pl

We show how the transverse  $\tau^+\tau^-$  spin correlations can be used to measure the parity of the Higgs boson and hence to distinguish a  $\mathcal{CP}$ -even  $H$  boson from  $\mathcal{CP}$ -odd  $A^0$  in the future high energy accelerator experiments. We investigate the subsequent decays of the  $\tau^\pm$  into  $\pi^\pm\bar{\nu}_\tau(\nu_\tau)$  and  $\rho^\pm\bar{\nu}_\tau(\nu_\tau)$ . The prospects for the measurement of the Higgs boson parity with a mass of 120 GeV are quantified for the case of  $e^+e^-$  collisions of 500 GeV center of mass energy. The Standard Model Higgsstrahlung production process is used as an example.

PACS numbers: 14.60.Fg, 14.80.Bn, 14.80.Cp

## 1. Introduction

In the Standard Model ( $\mathcal{SM}$ ) of elementary particle interactions, the breaking of electroweak symmetry is achieved through the Higgs mechanism. The simplest realization is provided by the introduction of a complex Higgs doublet, which leads to the presence of a neutral  $\mathcal{CP}$ -even Higgs boson in the physical spectrum. Among the possible extensions of the  $\mathcal{SM}$ , the Minimal Supersymmetric Standard Model ( $\mathcal{MSSM}$ ) has been considered most seriously. The minimal realization of the Higgs mechanism within supersymmetric extensions of the standard model requires the presence of two Higgs doublets at low energies. After the Higgs mechanism operates, five real fields remain, and there should be five spin zero Higgs fields, and the spectrum includes also a pseudoscalar  $\mathcal{CP}$ -odd state. This non trivial assignment of the quantum numbers requires the investigation of experimental

---

\* Presented at the Cracow Epiphany Conference on *Heavy Flavors*, 3-6 January 2003, Cracow.

\*\* Report-no: TTP03-13

opportunities to measure the parity of the Higgs boson states. The investigation of the mechanism of the electroweak symmetry breaking is one of the central task of a future  $e^+e^-$  linear collider operating at center-of-mass energies between 350 and 1000  $GeV$ . This accelerator will allow to study completely and with high accuracy also the profile of the Higgs sector.

The problem of the Higgs boson(s) parity measurement was approached in general form quite early in Ref. [1, 2] for Higgs decays into fermions and gauge boson pairs. It has recently been revived [3, 4, 5, 6, 7, 8, 9].

In this study we investigate the case of a Higgs boson which is light enough that the  $W^+W^-$  decay channel remains closed. Then the most promising decay channel of neutral Higgs particles is the  $b\bar{b}$  channel,  $\mathcal{BR}(H \rightarrow b\bar{b}) \sim 90\%$ . This applies in the  $\mathcal{SM}$  as well as in the minimal supersymmetric extension like  $\mathcal{MSSM}$  [10]. However, due to depolarization effects in the fragmentation process, it is very difficult to extract information on the  $b$  polarization state [11]. A much cleaner channel, though with branching ratios suppressed by an order of magnitude, is the  $\tau^+\tau^-$  mode,  $\mathcal{BR}(H \rightarrow \tau^+\tau^-) \sim 9\%$ . The  $\tau^+\tau^-$  channel is useful in the  $\mathcal{SM}$  for Higgs masses less than  $\sim 140\text{ GeV}$ . Up to this mass, the Higgs particle is very narrow,  $\Gamma(H) \leq 10\text{ MeV}$ . In Supersymmetric theories, the  $\tau^+\tau^-$  channel is useful over a much larger mass range. The main production mechanism of the  $\mathcal{SM}$  Higgs boson in  $e^+e^-$  collisions in the future Linear Collider ( $LC$ ) are the Higgsstrahlung process,  $e^+e^- \rightarrow ZH$  and the  $WW$  fusion process,  $e^+e^- \rightarrow W^*W^* \rightarrow \bar{\nu}_e\nu_e H$ . The cross section for the Higgsstrahlung process scales as  $\sim 1/s$  and dominates at low energies while the cross section for the  $WW$  fusion process rises as  $\sim \log(s/m_H^2)$  and dominates at high energies [10]. At  $\sqrt{s} = 500\text{ GeV}$ , the Higgsstrahlung and the  $WW$  fusion processes have approximately the same cross section for  $100\text{ GeV} \leq m_H \leq 200\text{ GeV}$ .

In our analysis, we will take as an example the  $e^+e^- \rightarrow ZH; Z \rightarrow \mu^+\mu^-$ ;  $H \rightarrow \tau^+\tau^-$  production process. We discuss a method for the parity measurement of the Higgs boson with a mass of  $120\text{ GeV}$  for the case of  $e^+e^-$  collisions with  $\sqrt{s} = 500\text{ GeV}$  using  $H/A^0 \rightarrow \tau^+\tau^-$ ;  $\tau^\pm \rightarrow \pi^\pm\bar{\nu}_\tau(\nu_\tau)$  and  $\tau^\pm \rightarrow \rho^\pm\bar{\nu}_\tau(\nu_\tau)$ ;  $\rho^\pm \rightarrow \pi^\pm\pi^0$  decay chains. All the Monte Carlo samples have been generated with the TAUOLA library [12, 13, 14]. For the production of the  $\tau$  lepton pairs the Monte Carlo program PYTHIA 6.1 is used [15]. The effects of initial state bremsstrahlung were included in the PYTHIA generation. For the  $\tau$  lepton pair decay with full spin effects included in the  $H \rightarrow \tau^+\tau^-$ ;  $\tau^\pm \rightarrow \pi^\pm\bar{\nu}_\tau(\nu_\tau)$  and  $\tau^\pm \rightarrow \rho^\pm\bar{\nu}_\tau(\nu_\tau)$ ;  $\rho^\pm \rightarrow \pi^\pm\pi^0$  chains, the interface explained in Refs. [16, 17] was used. It is an extended version of the standard universal interface of Refs. [18, 19].

The rest of the paper is organized as follows. In section 2 the theoretical considerations used to understand the decay chain of the Higgs particle are

explained. In section 3 and 4 we define the observables we use to distinguish between the scalar and pseudoscalar Higgs boson in the  $\tau^\pm \rightarrow \pi^\pm \bar{\nu}_\tau(\nu_\tau)$  and  $\tau^\pm \rightarrow \rho^\pm \bar{\nu}_\tau(\nu_\tau)$  decays respectively. In these sections we list our assumptions on detector effects and the imposed cuts as well as the main numerical results. A summary closes the paper.

## 2. Higgs boson parity

The  $H/A$  parity information must be extracted from the correlations between  $\tau^+$  and  $\tau^-$  spin components which are further reflected in correlations between the  $\tau$  decay products in the plane transverse to the  $\tau^+ \tau^-$  axes. This is because the decay probability, see *e.g.* Ref. [8],

$$\Gamma(H/A^0 \rightarrow \tau^+ \tau^-) \sim 1 - s_\parallel^{\tau^+} s_\parallel^{\tau^-} \pm s_\perp^{\tau^+} s_\perp^{\tau^-} \quad (1)$$

is sensitive to the  $\tau^\pm$  polarization vectors  $s^{\tau^-}$  and  $s^{\tau^+}$  (defined in their respective rest frames, the  $z$ -axis is oriented in the  $\tau^-$  flight direction). The symbols  $\parallel/\perp$  denote components parallel/transverse to the Higgs boson momentum as seen from the respective  $\tau^\pm$  rest frames. This suggests that the experimentally clean  $\tau^+ \tau^-$  final state may be the proper instrument to study the parity of the Higgs boson.

Now, a few representative examples of the  $\tau$  lepton decay will be discussed in more detail. In particular, we analyze the  $\tau$  decay into one and two pions.

## 3. Higgs $CP$ from $\tau^\pm \rightarrow \pi^\pm \bar{\nu}_\tau(\nu_\tau)$ decay

Exploring transverse spin correlations in the Higgs boson decay  $H/A^0 \rightarrow \tau^+ \tau^-; \tau^\pm \rightarrow \pi^\pm \bar{\nu}_\tau(\nu_\tau)$  one can provide a model independent parity determination test. The method relies on the properties of the Higgs boson Yukawa coupling to the  $\tau$  lepton, which in the general case can be written as  $\bar{\tau}(a_\tau + i b_\tau \gamma_5)\tau$ . The method does not depend on the Higgs boson production mechanism at all. Even though the  $\tau^\pm \rightarrow \pi^\pm \bar{\nu}_\tau(\nu_\tau)$  decay mode is rare,  $\mathcal{BR}(\tau \rightarrow \pi \nu_\tau) \sim 11\%$ , it may serve as a simple example that illustrates the basic principles.

The spin of the  $\tau^\pm$  leptons is not directly observable but translates directly into correlations among their decay products. To demonstrate this we define the polar angles between the  $\pi^\pm$  and the  $\tau^-$  direction in the  $\tau^\pm$  rest frames by  $\theta^\pm$  and the relative azimuthal angle  $\phi^*$  between the decay planes. The angular correlation between  $\tau^+ \tau^-$  decay products may then be

written as [20]

$$\frac{1}{\Gamma} \frac{d\Gamma(H/A^0 \rightarrow \pi^+ \bar{\nu}_\tau \pi^- \nu_\tau)}{d\cos\theta^+ d\cos\theta^- d\phi^*} = \frac{1}{8\pi} [1 + \cos\theta^- \cos\theta^+ \mp \sin\theta^+ \sin\theta^- \cos\phi^*]. \quad (2)$$

A simple asymmetry in the azimuthal angle that projects out the parity of the particle can be derived [1, 3] by integrating out the polar angles

$$\frac{1}{\Gamma} \frac{d\Gamma(H/A^0)}{d\phi^*} = \frac{1}{2\pi} \left[ 1 \mp \frac{\pi^2}{16} \cos\phi^* \right]. \quad (3)$$

A useful observable sensitive to the parity of the decaying Higgs particle is the angle  $\delta$  between the two charged pions in the Higgs boson rest frame [20]. This delicate measurement will require, however, the reconstruction of the Higgs boson rest-frame. It is generally accepted that the Monte Carlo method is the only way to estimate whether the measurement can be realized in practice, and which features of the future detection set up may turn out to be crucial. To enable such studies we have extended the standard universal interface [18, 19], of the **TAUOLA**  $\tau$ -lepton decay library [12, 13, 14], to include the complete spin effects for  $\tau$  leptons originating from the spin zero particle [16, 17]. The interface is expected to work with any Monte Carlo generator providing Higgs boson production, and subsequent decay into a pair of  $\tau$  leptons.

Let us turn to the discussion of numerical results. As an example we took a Higgs boson of 120 GeV. Fig. 1 presents the distribution in the angle  $\phi^* = \arccos(\vec{n}^+ \cdot \vec{n}^-)$  where

$$\vec{n}^\pm = \frac{\vec{p}^{\pi^\pm} \times \vec{p}^{\tau^-}}{|\vec{p}^{\pi^\pm} \times \vec{p}^{\tau^-}|}, \quad (4)$$

*i.e.* the acoplanarity angle. Thick lines will denote predictions for the scalar Higgs boson and thin lines for the pseudoscalar one. The distribution is indeed, as it should be, proportional to  $\sim 1 \mp \frac{\pi^2}{16} \cos\phi^*$  respectively for scalar and pseudoscalar Higgs boson, see Eq.(5). In Fig. 2 we plot the distribution of the  $\pi^+ \pi^-$  acollinearity angle ( $\delta^*$ ). The difference between the case of a scalar and a pseudoscalar Higgs boson is clearly visible, especially for acollinearities close to  $\pi$ .

To test the feasibility of the measurement, some assumptions about the detector effects have to be made. We include, as the most critical for our discussion, effects due to inaccuracies in the measurements of the  $\pi^\pm$  momenta. We assume Gaussian spreads of the ‘measured’ quantities with respect to the generated ones. For charged pion momentum we assume a 0.1% spread on its energy and direction.

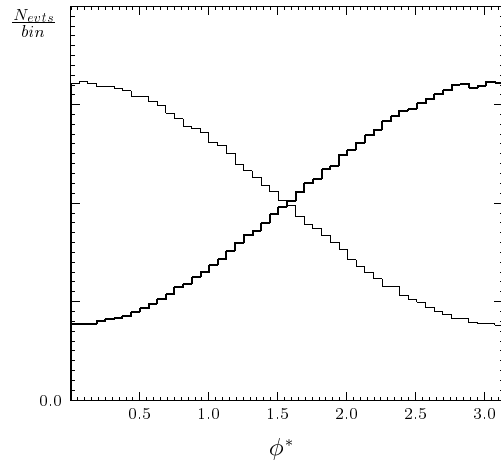


Fig. 1. The  $\pi^+\pi^-$  acoplanarity distribution (angle  $\phi^*$ ) in the Higgs boson rest frame. The thick line denotes the case of the scalar Higgs boson and thin line the pseudoscalar one.

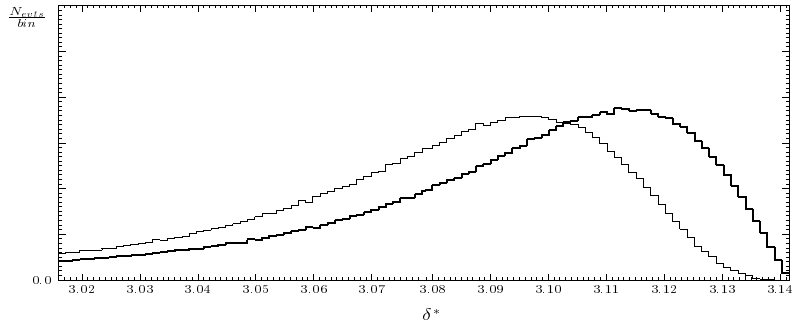


Fig. 2. The  $\pi^+\pi^-$  acollinearity distribution (angle  $\delta^*$ ) in the Higgs boson rest frame. Parts of the distribution close to the end of the spectrum;  $\delta^* \sim \pi$  are shown. No smearing is done. The thick line denotes the case of the scalar Higgs boson and the thin line the pseudoscalar one.

If the information on the beam energies and energies of all other observed particles (high  $p_T$  initial state bremsstrahlung photons, decay products of  $Z$  etc.) are taken into consideration the Higgs boson rest frame can be reconstructed. We may define the “reconstructed” Higgs boson momentum as the difference of the sum of the beam energies and the momenta of all visible particles, that is decay products of the  $Z$  and all radiative photons of  $|\cos \theta| < 0.98$ . In our study we will mimic in a very crude way the beamstrahlung effects, assuming only a flat spread over the range of  $\pm 5$   $GeV$  for the longitudinal component of the Higgs boson momentum with respect to the generated one<sup>1</sup>.

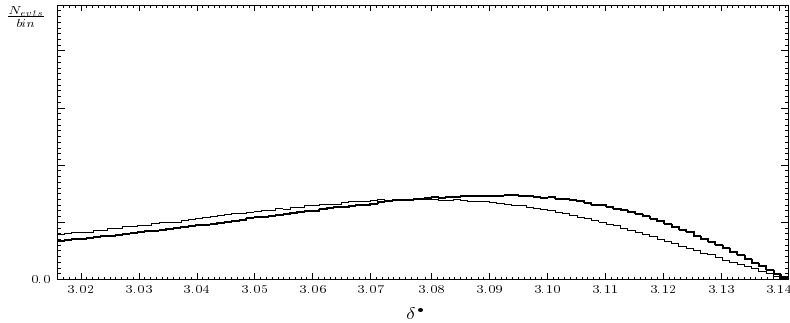


Fig. 3. The  $\pi^+\pi^-$  acollinearity distribution (angle  $\delta^\bullet$ ) in the reconstructed Higgs boson rest frame. All smearing is included. Parts of the distribution close to the end of the spectrum;  $\delta^\bullet \sim \pi$  are shown. The thick line denotes the case of the scalar Higgs boson and the thin line the pseudoscalar one.

Fig. 3 shows us the distribution of the acollinearity angle ( $\delta^\bullet$ ) build from smeared  $\pi^\pm$  momenta defined in the reconstructed Higgs boson rest-frame. The difference between the scalar and the pseudoscalar Higgs bosons is only barely visible. We have studied several mechanisms of Higgs boson production, in all cases depletion of the acollinearity distribution sensitivity to transverse spin effect was quite similar. We can conclude that our results are thus independent from the production mechanism.

The beamstrahlung effect taken into account in the reconstruction of the Higgs boson four-momentum degraded the method of measuring the Higgs

<sup>1</sup> The typical spread for the beam energy in a linear collider is of the order of a few percent [21].

boson parity using the decay chain  $H \rightarrow \tau^+ \tau^-$ ,  $\tau^\pm \rightarrow \pi^\pm \bar{\nu}_\tau(\nu_\tau)$  in a decisive way. Therefore, there is little hope for the elegant method to check the Higgs boson parity using its decay to  $\tau^\pm \rightarrow \pi^\pm \bar{\nu}_\tau(\nu_\tau)$ , whatever the luminosity of the future Linear Collider is assumed, unless other, unfortunately less sensitive, to spin, than  $\tau^\pm \rightarrow \pi^\pm \bar{\nu}_\tau(\nu_\tau)$ , decay modes are used as well.

#### 4. Higgs $CP$ from $\tau^\pm \rightarrow \rho^\pm \bar{\nu}_\tau(\nu_\tau)$ decay

The discussion of the  $\tau$  decay to a two pion final state follows very much the same line. We may treat the hadron system as a single particle with definite spin and mass,  $m_\rho = \sqrt{Q^2}$ , or we may extract additional information from the individual pion momenta. The first strategy leads to a simple generalization of the single pion case. However, the effect is diminished as compared with the  $\tau^\pm$  decays to single  $\pi^\pm \bar{\nu}_\tau(\nu_\tau)$ . This is because for the  $\tau^\pm \rightarrow \rho^\pm \bar{\nu}_\tau(\nu_\tau)$  decay the angular correlation term is reduced by the factor  $(m_\tau^2 - 2Q^2)^2 / (m_\tau^2 + 2Q^2)^2$

$$\frac{1}{\Gamma} \frac{d\Gamma(H/A^0 \rightarrow \rho^+ \bar{\nu}_\tau \rho^- \nu_\tau)}{d \cos \theta^+ d \cos \theta^- d\phi^*} = \frac{1}{8\pi} \left[ 1 + \frac{(m_\tau^2 - 2Q^2)^2}{(m_\tau^2 + 2Q^2)^2} [\cos \theta^- \cos \theta^+ \mp \sin \theta^+ \sin \theta^- \cos \phi^*] \right]. \quad (5)$$

The mass of the hadronic system,  $Q^2$ , can no longer be neglected relative to  $m_\tau^2$  [22].

Let us turn to the case when additional information coming from  $\rho^\pm$  decay products can be used directly [17]. The  $\tau^\pm \rightarrow \rho^\pm \bar{\nu}_\tau(\nu_\tau)$  decay is very interesting because it has, by far, the largest branching ratio,  $\mathcal{BR}(\tau \rightarrow \rho \nu_\tau) \sim 25\%$ . The polarimetric force of this channel can be improved if information on the  $\rho$  decay products, *i.e.* on details of the decay  $\tau^\pm \rightarrow \pi^\pm \pi^0 \bar{\nu}_\tau(\nu_\tau)$ , is used. This is of no surprise because the polarimetric vector is given by the formula

$$h^i = \mathcal{N} (2(q \cdot N)q^i - q^2 N^i) \quad (6)$$

where  $\mathcal{N}$  is a normalization function,  $q$  is the difference of the  $\pi^\pm$  and  $\pi^0$  four-momenta and  $N$  is the four-momentum of the  $\tau$  neutrino (all defined in the  $\tau$  rest frame) see, *e.g.* [12]. Obviously, any control on the vector  $q$  can be advantageous. It is of interest to note that in the  $\tau$  lepton rest frame, when  $m_{\pi^\pm} = m_{\pi^0}$  is assumed, the term

$$q \cdot N = (E_{\pi^\pm} - E_{\pi^0})m_\tau. \quad (7)$$

Thus, to exploit this part of the polarimetric vector, we need to have some handle on the difference of the  $\pi^\pm$  and  $\pi^0$  energies in their respective  $\tau^\pm$  leptons rest frames. Otherwise, the effect of this part of the polarimetric vector cancels out and one is left with the part proportional to the  $\rho$  (equivalently  $\nu_\tau$ ) momentum.

Let us now discuss a new observable which we have introduced to distinguish between the scalar and the pseudoscalar Higgs boson. We advocate the observable where we ignore the part of the polarimetric vector proportional to the  $\rho^\pm$  (equivalently  $\nu_\tau$ ) momentum in the  $\tau$  rest frame. We rely only on the part of the vector due to the differences of the  $\pi^\pm$  and  $\pi^0$  momenta, which manifests the spin state of the  $\rho^\pm$ . In the Higgs boson rest frame the  $\rho$  momentum represents a larger fraction of the Higgs's energy than the neutrino. Therefore, we abandon the reconstruction of the Higgs boson rest frame and instead we use the  $\rho^+\rho^-$  rest frame which has the advantage that it is built only from directly visible decay products of the  $\rho^+$  and  $\rho^-$ . In the rest frame of the  $\rho^+\rho^-$  system we define the acoplanarity angle,  $\varphi^*$ , between the two planes spanned by the immediate decay products (the  $\pi^\pm$  and  $\pi^0$ ) of the two  $\rho$ 's, see Fig. 4.

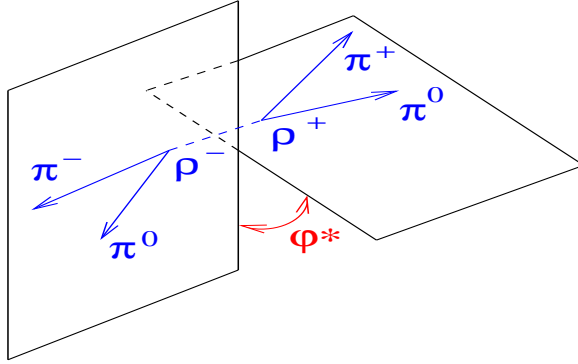


Fig. 4. *Definition of the  $\rho^+\rho^-$  decay products' acoplanarity distribution angle,  $\varphi^*$  in the rest frame of the  $\rho^+\rho^-$  pair.*

The variable  $\varphi^*$  alone does not distinguish the scalar and pseudoscalar Higgs boson. To do this we must go further. The  $\tau^\pm \rightarrow \pi^\pm \pi^0 \bar{\nu}_\tau (\nu_\tau)$  spin sensitivity is proportional to the energy difference of the charged and neutral pion (in the  $\tau$  rest frame), see formula (7). We have to separate events into two zones,  $C$  and  $D$ ,

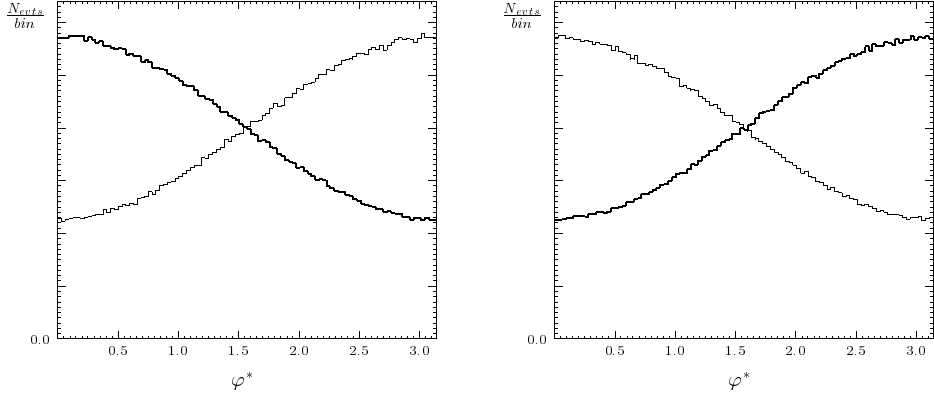


Fig. 5. The  $\rho^+\rho^-$  decay products' acoplanarity distribution angle,  $\varphi^*$ , in the rest frame of the  $\rho^+\rho^-$  pair. A cut on the differences of the  $\pi^\pm\pi^0$  energies defined in their respective  $\tau^\pm$  rest frames to be of the same sign, selection  $y_1y_2 > 0$ , is used in the left plot and the opposite sign, selection  $y_1y_2 < 0$ , is used for the right plot. No smearing is done. Thick lines denote the case of the scalar Higgs boson and thin lines the pseudoscalar one.

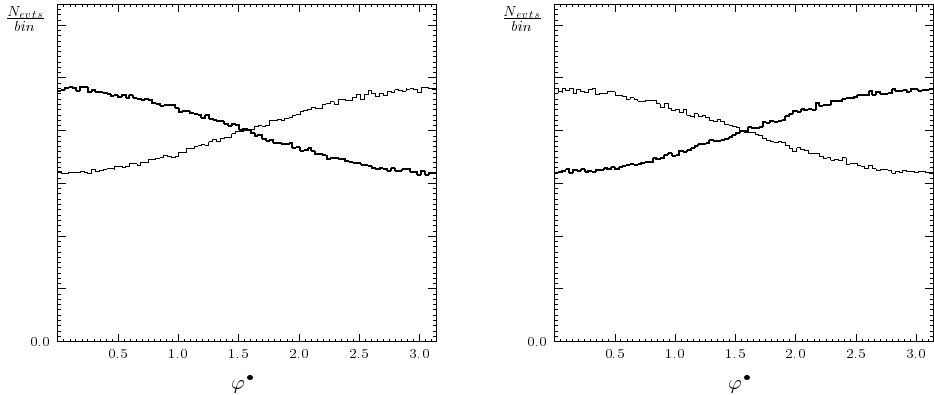


Fig. 6. The  $\rho^+\rho^-$  decay products' acoplanarity distribution angle,  $\varphi^\bullet$ , in the rest frame of the  $\rho^+\rho^-$  pair. A cut on the differences of the  $\pi^\pm\pi^0$  energies defined in their respective replacement  $\tau^\pm$  rest frames to be of the same sign, selection  $y_1y_2 > 0$ , is used in the left plot and the opposite sign, selection  $y_1y_2 < 0$ , is used for the right plot. All smearing is included. Thick lines denote the case of the scalar Higgs boson and thin lines the pseudoscalar one.

$$C : \quad y_1 y_2 > 0$$

$$D : \quad y_1 y_2 < 0$$

where,

$$y_1 = \frac{E_{\pi^+} - E_{\pi^0}}{E_{\pi^+} + E_{\pi^0}} ; \quad y_2 = \frac{E_{\pi^-} - E_{\pi^0}}{E_{\pi^-} + E_{\pi^0}}. \quad (8)$$

$E_{\pi^\pm}$  and  $E_{\pi^0}$  are the  $\pi^\pm, \pi^0$  energies in the respective  $\tau^\pm$  rest frames.

In Fig. 5 we plot the distribution of  $\varphi^*$ , where the left hand plot contains the events where the energy difference between the  $\pi^+$  and  $\pi^0$  defined in the  $\tau^+$  rest frame is of the same sign as the energy difference of  $\pi^-$  and  $\pi^0$  defined in  $\tau^-$  rest frame (selection  $y_1 y_2 > 0$ ). The right hand plot contains the events with the opposite signs for the two energy differences (selection  $y_1 y_2 < 0$ ). It can be seen that the differences between the scalar and pseudoscalar Higgs boson are large. If the energy difference cut was not applied, we would have completely lost sensitivity to the Higgs boson parity.

Unfortunately, since the  $\tau$ -lepton is not measurable, such a selection cut cannot be used directly. We reconstruct the  $\tau$  lepton rest frames, and we assume Gaussian spreads of the ‘measured’ quantities with respect to the generated ones. For charged pion momentum we assume a 0.1% spread on its energy and direction. For neutral pion momentum we assume an energy spread of  $\frac{5\%}{\sqrt{E[GeV]}}$ . For the  $\theta$  and  $\phi$  angular spread we assume  $\frac{1}{3} \frac{2\pi}{1800}$ . These neutral pion resolutions can be achieved with a 15% energy error and a  $2\pi/1800$  direction error in the gammas resulting from the  $\pi^0$  decays. These resolutions have been approximately verified with a **SIMDET** [23], a parametric Monte Carlo program for a TESLA detector [24]. In Ref. [17] the method of reconstruction of replacement  $\tau^\pm$  lepton rest frames was proposed. We will use this method here as well. We boost the  $\pi^+, \pi^0, \pi^-, \pi^0$  momenta to the respective replacement  $\tau^\pm$  lepton rest frames. The  $\pi^\pm$  energies defined this way are used in the  $y_1$  and  $y_2$  energy difference cuts.

When we use the selection cuts  $y_1$  and  $y_2$  and the replacement  $\tau^\pm$  rest frames as well as smearing the  $\pi^\pm$  momenta, we obtain the results shown in Fig. 6. We see that the effects to be measured diminish but remain clearly visible.

### Summary

We have studied the possibility of distinguishing a scalar from a pseudoscalar couplings of light Higgs boson to fermions using its decay to a

pair of  $\tau^+\tau^-$  leptons and their subsequent decays to  $\tau^\pm \rightarrow \pi^\pm \bar{\nu}_\tau(\nu_\tau)$  and  $\tau^\pm \rightarrow \rho^\pm \bar{\nu}_\tau(\nu_\tau)$ ;  $\rho^\pm \rightarrow \pi^\pm \pi^0$ .

The beamstrahlung effect in reconstruction of the Higgs boson four-momentum degraded the method of measuring the Higgs boson parity using the decay chain  $H \rightarrow \tau^+\tau^-$ ,  $\tau^\pm \rightarrow \pi^\pm \bar{\nu}_\tau(\nu_\tau)$  in a decisive way. Therefore, there is little hope for the elegant method to check Higgs boson parity using its decay to  $\tau^\pm \rightarrow \pi^\pm \bar{\nu}_\tau(\nu_\tau)$ , whatever the luminosity of the future Linear Collider is assumed.

For  $\tau^\pm \rightarrow \rho^\pm \bar{\nu}_\tau(\nu_\tau)$  decay, we have discussed an observable which is very promising. Using reasonable assumptions about the  $\mathcal{SM}$  production cross section and about the measurement resolutions we find that with 500  $fb^{-1}$  of luminosity at a 500  $GeV$   $e^+e^-$  linear collider the  $\mathcal{CP}$  of a 120  $GeV$  Higgs boson can be measured to a confidence level greater than 95%. We emphasize that the technique is both model independent and independent of the Higgs boson production mechanism and depends only on good measurements of the Higgs boson decay products. Thus, this method may be applicable to other production modes including those available at proton colliders as well as at electron colliders.

### Acknowledgments

It is a pleasure to thank Gary Bower, Tomasz Pierzchała and Zbigniew Wąs, with whom the work reported here was performed. I wish to thank Marek Jeżabek for giving me the opportunity to give this talk at the Cracow Epiphany Conference on Heavy Flavors. This work is partly supported by the Polish State Committee for Scientific Research (KBN) grants Nos 5P03B09320, 2P03B00122.

### REFERENCES

- [1] J. R. Dell'Aquila and C. A. Nelson, *Nucl. Phys.* **B320** (1989) 61.
- [2] J. R. Dell'Aquila and C. A. Nelson, *Nucl. Phys.* **B320** (1989) 86.
- [3] V. Barger, K. Cheung, A. Djouadi, B. A. Kniehl, and P. M. Zerwas, *Phys. Rev.* **D49** (1994) 79, [hep-ph/9306270](#).
- [4] K. Hagiwara and M. Stong, *Z. Phys.* **C62** (1994) 99, [hep-ph/9309248](#).
- [5] A. Skjold and P. Osland, *Phys. Lett.* **B329** (1994) 305, [hep-ph/9402358](#).
- [6] C. A. Boe, O. M. Ogreid, P. Osland, and J. Z. Zhang, *Eur. Phys. J.* **C9** (1999) 413, [hep-ph/9811505](#).
- [7] K. Hagiwara, S. Ishihara, J. Kamoshita, and B. Kniehl, *Eur. Phys. J.* **C14** (2000) 457, [hep-ph/0002043](#).

- [8] M. Kramer, J. H. Kühn, M. L. Stong, and P. M. Zerwas, *Z. Phys.* **C64** (1994) 21, [hep-ph/9404280](#).
- [9] B. Grzadkowski and J. F. Gunion, *Phys. Lett.* **B350** (1995) 218, [hep-ph/9501339](#).
- [10] J. A. Aguilar-Saavedra *et al.*, "TESLA Technical Design Report Part III: Physics at an  $e^+e^-$  Linear Collider", [hep-ph/0106315](#).
- [11] B. Mele and G. Altarelli, *Phys. Lett.* **B299** (1993) 345.
- [12] S. Jadach, J. H. Kühn, and Z. Wąs, *Comput. Phys. Commun.* **64** (1990) 275.
- [13] M. Jeżabek, Z. Wąs, S. Jadach, and J. H. Kühn, *Comput. Phys. Commun.* **70** (1992) 69.
- [14] S. Jadach, Z. Wąs, R. Decker, and J. H. Kühn, *Comput. Phys. Commun.* **76** (1993) 361.
- [15] T. Sjostrand *et al.*, *Comput. Phys. Commun.* **135** (2001) 238, [hep-ph/0010017](#).
- [16] Z. Wąs and M. Worek, *Acta Phys. Polon.* **B33** (2002) 1875, [hep-ph/0202007](#).
- [17] G. R. Bower, T. Pierzchała, Z. Wąs, and M. Worek, *Phys. Lett.* **B543** (2002) 227–234, [hep-ph/0204292](#).
- [18] T. Pierzchała, E. Richter-Wąs, Z. Wąs, and M. Worek, *Acta Phys. Polon.* **B32** (2001) 1277, [hep-ph/0101311](#).
- [19] M. Worek, *Acta Phys. Polon.* **B32** (2001) 3803, [hep-ph/0110228](#).
- [20] J. H. Kühn and F. Wagner, *Nucl. Phys.* **B236** (1984) 16.
- [21] ACFA Linear Collider Working Group Collaboration, "Particle physics experiments at JLC", [hep-ph/0109166](#).
- [22] Particle Data Group Collaboration, K. Hagiwara *et al.*, *Phys. Rev.* **D66** (2002) 010001.
- [23] M. Pohl and H. J. Schreiber, "SIMDET - Version 4: A parametric Monte Carlo for a TESLA detector", [hep-ex/0206009](#).
- [24] T. Behnke, S. Bertolucci, R. D. Heuer, and R. Settles, "TESLA Technical Design Report Part IV: A detector for TESLA", DESY-01-011.